

Neutralino Dark Matter at 14 TeV and 100 TeV

Matthew Low and Lian-Tao Wang

Department of Physics, Enrico Fermi Institute, and Kavli Institute for Cosmological Physics, University of Chicago, Chicago, IL 60637

E-mail: mattlow@uchicago.edu, liantaow@uchicago.edu

ABSTRACT: In recent years the search for dark matter has intensified with competitive bounds coming from collider searches, direct detection, and indirect detection. Collider searches at the Large Hadron Collider (LHC) lack the necessary center-of-mass energy to probe TeV-scale dark matter. It is TeV-scale dark matter, however, that remains viable for many models of supersymmetry. In this paper, we study the reach of a 100 TeV proton-proton collider for neutralino dark matter and compare to 14 TeV LHC projections. We employ a supersymmetric simplified model approach and present reach estimates from monojet searches, soft lepton searches, and disappearing track searches. The searches are applied to pure neutralino spectra, compressed neutralino spectra, and coannihilating spectra. We find a factor of 4-5 improvement in mass reach in going from 14 TeV to 100 TeV. More specifically, we find that given a 1% systematic uncertainty, a 100 TeV collider could exclude winos up to 1.4 TeV and higgsinos up to 850 GeV in the monojet channel. Coannihilation scenarios with gluinos can be excluded with neutralino masses of 6.2 TeV, with stops at 2.8 TeV, and with squarks at 4.0 TeV. Using a soft lepton search, compressed spectra with a chargino-neutralino splitting of $\Delta m = 20 - 30$ GeV can exclude neutralinos at ~ 1 TeV. Given a sufficiently long chargino lifetime, the disappearing track search is very effective and we extrapolate current experimental bounds to estimate that a ~ 2 TeV wino could be discovered and a ~ 3 TeV wino could be excluded.

Contents

1	Introduction	1
2	Analysis Overview	3
3	Pure Wino	5
4	Pure Higgsino	9
5	Mixed Spectra	11
6	Coannihilating Spectra	15
7	Conclusions	18
A	Analysis Details	21
B	Extrapolating Systematics	24

1 Introduction

The existence of cold dark matter is one of very few pieces of experiment evidence for physics beyond the standard model [1]. Its identity, however, remains one of the most outstanding questions in particle physics. Among the myriad possibilities, a weakly interacting massive particle (WIMP) is one of the most compelling. The WIMP scenario assumes that dark matter has weak, but still sizable interactions with the standard model. The cross-section for a pair of WIMPs interacting with a pair of standard model particles can be written as $\sigma \propto g_{\text{eff}}^4/M_{\text{DM}}^2$, where g_{eff} is the effective coupling characterizing the interaction. To avoid overclosing the universe, we must have

$$M_{\text{DM}} \lesssim 1.8 \text{ TeV} \left(\frac{g_{\text{eff}}^2}{0.3} \right). \quad (1.1)$$

Thus the WIMP mass is expected to be near the weak scale, which offers the exciting prospect of discovery at on-going or future collider experiments.

It is certainly possible that dark matter is part of a complete TeV-scale new physics model which contains other new particles that do not comprise the dark matter content of the universe. Low energy supersymmetry (SUSY) is one of the most prominent examples [2, 3]. In the usual naturalness-motivated SUSY scenarios, all of the superpartners are relatively light and the lightest superpartner (LSP) is stable and makes up the full dark matter content of the universe. As stringent constraints already exist on the properties of dark matter, including it be neutral and uncolored, in the minimal supersymmetric standard model (MSSM) the identity of the LSP is the lightest neutralino. At hadron colliders such as the Large Hadron Collider (LHC), the pair production of colored superpartners, squarks and gluinos, are the dominant SUSY processes. The squarks or gluinos then decay both to standard model particles and the LSP via a, possibly long, decay chain. The standard SUSY searches designed for this scenario look for jets and missing energy and would discover dark matter along with other superpartners [4–6]. Thus the mass reach for dark matter is strongly correlated with that of gluinos and squarks. Due to kinematics, the mass reach for the LSP is typically weaker by a few hundred GeV.

Concurrently with complete models, it is also crucial to explore the discovery potential for dark matter independent of the presence of additional new particles. The starting point here would be to consider a set of simple examples of possible dark matter candidates. Since dark matter cannot be electrically charged, the simplest possibility is a dark matter particle as the neutral member of a standard model weak multiplet. WIMPs, as their name suggests, fall into this category. Neutralino dark matter, in fact, already provides concrete realizations of three of the simplest cases. The higgsino is a vector-like doublet, the wino is a triplet, and the bino provides an example of a singlet which can mix with the other multiplets after electroweak symmetry breaking. Therefore, as a first step to directly studying dark matter, we choose to consider dark matter as a neutralino LSP. In general, except in coannihilation scenarios, we will assume all other squarks and sleptons are too heavy to be relevant for dark matter production at colliders. These have been called simplified models of dark matter and are similar to the split SUSY scenario [7–9].

As we employ simplified models, the basic collider process is simply dark matter pair production. As dark matter will escape the detector unseen, there needs to be additional hard radiation of a standard model particle, which could be a quark or gluon [10, 11], photon [12, 13], W [14] or Z [15, 16], or even a higgs [17–19]. Among them, a quark or gluon emission, the *monojet* channel, is typically the most sensitive. When the LSP is a mixed state, the LSP can be separated by a mass splitting $\Delta m \equiv m_{\tilde{\chi}_1^\pm} - m_{\tilde{\chi}_1^0} \sim 20 - 50$ GeV from the other chargino and neutralino states. In this case, in addition to a hard jet, it is possible to search for low p_T leptons resulting from a chargino or neutralino which decays to the LSP and leptons or quarks. We call this the *soft lepton* channel. When the LSP is a pure state, at tree-level it is mass degenerate with the charged components. As the mass splitting is generated at loop-level, it is small and can lead to charginos with a macroscopic lifetime. This leaves a rather striking signature of high p_T charged track abruptly ending when the chargino decays

to the LSP and very soft, likely undetected, standard model particles. We also include this *disappearing tracks* search in our consideration.

Since typically only a small fraction of the center of mass energy of a hadron collider is available in hard collisions, we expect only a small part of the WIMP parameter space, shown in Eq. 1.1, can be probed at the 14 TeV LHC. This has been confirmed by a number of recent studies [20–24]. In our study, we focus on the prospects at a 100 TeV proton-proton collider [5, 25]. For comparison, we will also often show results for the 14 TeV LHC.

We briefly outline our simulation procedure and sketch the analyses implemented in Sect. 2. We then present results for pure wino dark matter and pure higgsino dark matter in Sect. 3 and Sect. 4, respectively. Mixed scenarios are shown in Sect. 5, as well as coannihilation spectra in Sect. 6. Finally our conclusions are summarized in Sect. 7. The first appendix, App. A, provides a more comprehensive description of the analyses and the second appendix, App. B, includes a brief discussion on the dominant systematic uncertainties.

2 Analysis Overview

In this section we give a brief overview of how we simulated events and the various analyses applied. A more thorough discussion is found in App. A. The SUSY mass spectra were computed with Suspect2 [26] using parameters input at the weak-scale with $\tan\beta = 20$. Events were generated using MadGraph 5 v1.5.12 [27] for matrix elements and Pythia 6 [28] for showering and hadronization. All signals and backgrounds were matched up to two additional jets using the MLM matching scheme (except for $t\bar{t}$ which was matched to one additional jet). Delphes 3 v3.0.9 [29] was used as a detector simulation with the Snowmass detector card [30–32]. The Snowmass Delphes settings identify electrons and muons above 10 GeV, tag hadronic tau leptons with an efficiency of 65%, and cluster anti- k_T jets [33] with a radius of $R = 0.5$ using Fastjet v3.0.3 [34].

The inclusive pair production cross-sections were verified using Prospino 2 [35] for pure spectra. While the k-factors are known for the $2 \rightarrow 2$ process, a collider search requires there be a hard visible object to trigger on corresponding to the $2 \rightarrow 3$ process. The k-factor for this process is not the same as the $2 \rightarrow 2$ process. In fact, since going to next-to-leading order from leading-order opens up different new partonic channels for the $2 \rightarrow 2$ and $2 \rightarrow 3$ processes, we should expect the pair production k-factor to differ from k-factor for the monojet search [36]. In this study we choose not to apply k-factors on the signal or background. As the signal cross-section falls very quickly with mass, we expect neglecting k-factors to only introduce a small error.

Monojet

The first analysis we implement looks for one hard jet produced with large missing energy (\cancel{E}_T), known as a monojet search. Monojet searches have been carried out both at the Tevatron [37–39] and the LHC [40–43] looking both for large extra dimensions and dark

matter via a contact operator [10, 11] or light mediator [44–46]. We follow the format of the most recent CMS analysis which uses 19.5 fb^{-1} of 8 TeV data [43]. The CMS search requires one or two hard jets, where the second jet cannot be back-to-back with the first jet, and large \cancel{E}_T . Events that contain electrons, muons, or tagged hadronic taus are vetoed.

The backgrounds for this channel include standard model processes with a hard jet and neutrinos. Despite the lepton veto, processes with leptons also comprise part of the background because leptons can fail to be tagged if they are outside the detector acceptance, not isolated, or too soft. This leads to a long list of backgrounds: $Z(\nu\nu) + \text{jets}$, $W(\ell\nu) + \text{jets}$, $t\bar{t}$, $Z(\ell\ell) + \text{jets}$, single t , diboson production, and QCD multijets¹. Of these, only $Z(\nu\nu) + \text{jets}$ is irreducible and it comprises roughly 70% of the background in the signal region. Together with $W(\ell\nu) + \text{jets}$ these backgrounds make up 99% of the background. For completeness we generate $Z(\nu\nu) + \text{jets}$, $W(\ell\nu) + \text{jets}$, $t\bar{t}$, $Z(\ell\ell) + \text{jets}$, and $W(\ell\nu)W(\ell\nu) + \text{jets}$ backgrounds with MadGraph.

Soft Leptons

When the LSP is split from other electroweakino states by $\Delta m = 20 - 50 \text{ GeV}$ then these states can also be pair produced and decay to the LSP via off-shell gauge bosons which decay hadronically or into low p_T leptons. The hadronic decays are difficult to extricate from the busy hadronic environment, but it is possible to tag the soft leptons. This is different from the standard multilepton searches [47–51] where there are both more and harder leptons. It has been noted in [52, 53] that triggering on a hard jet, as in the monojet search, is advantageous in a soft lepton search. As the optimal search strategy strongly depends on the electroweakino splittings, it would be interesting to look at the transition between a pure monojet search yielding the highest significance and a traditional multilepton search yielding the highest significance. This is beyond the scope of this note, and we restrict ourselves to the compressed region where $\Delta m = 20 - 30 \text{ GeV}$.

As in the monojet search, events are required to have one or two jets that are not back-to-back and large missing energy. Rather than applying a lepton veto, events are binned according to whether they contain 0, 1, or 2 soft leptons. The significances are computed separately in each lepton bin and added in quadrature. The backgrounds are the same as the monojet search, but the background composition varies significantly across lepton bins. Like the monojet channel, the 0-lepton bin is about 99% composed of $Z(\nu\nu) + \text{jets}$ and $W(\ell\nu) + \text{jets}$. The 1-lepton bin is more than 90% from $W(\ell\nu) + \text{jets}$ and the 2-lepton bin is dominated by $W(\ell\nu)W(\ell\nu) + \text{jets}$ at roughly 70% with the rest coming from $Z(\ell\ell) + \text{jets}$ and $t\bar{t}$.

Disappearing Tracks

The third analysis leverages the fact that in scenarios with dark matter as a pure state, a chargino are often near-degenerate with the LSP. In the limit $m_Z/m_{\tilde{\chi}} \rightarrow 0$, a pure wino

¹While QCD multijet events do not contain real missing energy, mismeasured jets can fake missing energy. As the multijet rate is dominated by dijet events requiring events with two jets to not be back-to-back effectively removes the QCD background.

has a splitting of ≈ 166 MeV and a pure higgsino has a splitting of ≈ 355 MeV [54, 55]. Due to the small mass splitting, the dominant decay $\tilde{\chi}^\pm \rightarrow \pi^\pm + \tilde{\chi}^0$ has a long lifetime. Thus, a fraction of the charginos can live long enough, $c\tau \sim 6$ cm, to leave a track in the inner detector. A number of phenomenological studies have been done [54, 56–63]. This is a promising search channel with no obvious physics background. One possibility is to look for so-called disappearing tracks, in which a chargino decays in the inner detector, resulting in a track that disappears where the chargino decays into a neutralino and a soft pion².

We derive our projections from a recent ATLAS search that reported a 95% exclusion limit close to 250 GeV, using 20.3 fb^{-1} of 8 TeV data [64]. Similar to the monojet analysis, this search triggers on a hard jet and large \cancel{E}_T , additionally requiring a disappearing track. While the monojet analysis has not yet reached the sensitivity necessary to probe the pure wino or pure higgsino scenarios, the disappearing track search is already starting to exclude regions of the pure wino parameter space. Therefore it is reasonable to expect that this channel will be much stronger both in the 14 TeV LHC run and at a 100 TeV proton-proton collider.

The significance of a given search is calculated as

$$\text{Significance} = \frac{S}{\delta B} = \frac{S}{\sqrt{B + \lambda^2 B^2 + \gamma^2 S^2}}, \quad (2.1)$$

where λ and γ parameterize the systematic uncertainty on the background and on the signal, respectively. While we assume the systematics are the same across background channels, considering different systematics for each background would not noticeably change the results, as each search is dominated by one or two backgrounds.

Our analyses have not included effects from pileup. As a future high energy proton-proton collider will likely operate with high instantaneous luminosity, events will contain a high level of hadronic contamination from pileup. In a fully realistic projection it is important to consider the effects of pileup and the effects of applying the appropriate pileup removal techniques [65–67]. For the analyses presented in this paper, however, events are selected with a very hard cut on the leading jet and missing energy so we expect such additional considerations will not significantly alter the results.

3 Pure Wino

The first set of SUSY spectra we consider are those with a pure wino LSP. This scenario can be realized if anomaly mediation the main mechanism through which the gaugino soft masses are generated [68, 69]. Models which implement this, along with the feature that the scalar

²The signature has also been called *kinked tracks* or *track stubs*. It is worth noting that this signal is part of a larger class of signatures of particles that traverse macroscopic distances before decaying. While it is detector-dependent, roughly speaking charged particles with a lifetime $c\tau = \mathcal{O}(\text{mm})$ result in displaced vertices, charged particles with a lifetime $c\tau = \mathcal{O}(\text{cm})$ result in disappearing tracks, and charged particles with a lifetime $c\tau = \mathcal{O}(\text{m})$ result in stable charged massive particles.

are heavy (compared to the gravitino mass) include split SUSY [7–9, 70], mini-split susy [71], and spread susy [72, 73].

For a wino LSP to thermally saturate the relic density, it must have a mass of $m_{\tilde{\chi}} \sim 3.1$ TeV (including the Sommerfeld effect) [74–76]. Assuming an NFW halo profile, current indirect detection experiments like Fermi [77] and HESS [78] constrain thermally produced winos to have a mass $m_{\tilde{\chi}} \lesssim 1.6$ TeV³. Future independent detection experiments, like CTA, could move this bound down to $m_{\tilde{\chi}} \lesssim 1.1$ TeV [79, 80]. These limits, however, are subject to a number of astrophysics uncertainties. Choosing different halo profile can move the HESS limit as low as $m_{\tilde{\chi}} \sim 0.5$ TeV and as high as $m_{\tilde{\chi}} \sim 2.2$ TeV [75]. Non-thermally produced, but relic density saturating, winos are ruled out across the parameter space up to $m_{\tilde{\chi}} \lesssim 25$ TeV.

Direct detection is another avenue through winos could be discovered. In the heavy wino limit, the spin-independent scattering cross-section has been calculated to be $\sigma_{\text{SI}} = 1.3 \times 10^{-47}$ cm² [81]. Future experiments are projected to probe this cross-section for dark matter masses of a few hundred GeV [82]. TeV-scale dark matter is not only beyond the predicted reach, but also sits along the neutrino coherent scattering floor [82].

As direct detection cannot probe thermally-saturating winos and indirect detection involves astrophysics uncertainties, there is a potentially interesting window in parameter space left open. As will be shown, the LHC will not be able to cover it, as it is only sensitive to $m_{\tilde{\chi}} \sim 280 - 380$ GeV winos. A 100 TeV collider, on the other hand, may be able to reach 1.4 – 2.9 TeV and cover the parameter space.

The wino is an electroweak triplet which results in one neutral and one charged state at low energies. The pair production of charginos proceeds via the Drell-Yan-like process of an s -channel Z going to a pair of charginos, which subsequently decay to the LSP and soft standard model particles. Charginos can also be produced directly along with a neutralino via an s -channel W^{\pm} .

The mass reach in the monojet channel for a pure wino LSP is shown in Fig. 1. The significance is computed using Eq. 2.1. We set $\gamma = 10\%$, although its value has a very small effect since $S \ll B$ in much of the parameter space we explore. The value of λ is varied between 1 – 2%, which generates the bands in the plot. In the large background limit Eq. 2.1 is $\approx (1/\lambda)(S/B)$, which means varying λ by a factor of 2 can vary the significance by up to a factor of 2. While the impact of background systematic uncertainty is clear, it is difficult to exactly project the systematic uncertainty of a future detector. Naively scaling the current systematics in [43] with luminosity would result in $\approx 0.5\%$ for 3000 fb⁻¹. This is likely much too optimistic as components of the systematic uncertainty do not scale with statistics. While even 1 – 2% may be overly optimistic, this at least provides a benchmark. Given the importance of the monojet channel in the search for dark matter, not just in the pure wino case, minimizing possible systematics is a salient factor to be included in the design of detectors at future hadron colliders.

³Thermally produced winos with a mass $m_{\tilde{\chi}} \lesssim 3.1$ TeV would only comprise part of the relic abundance.

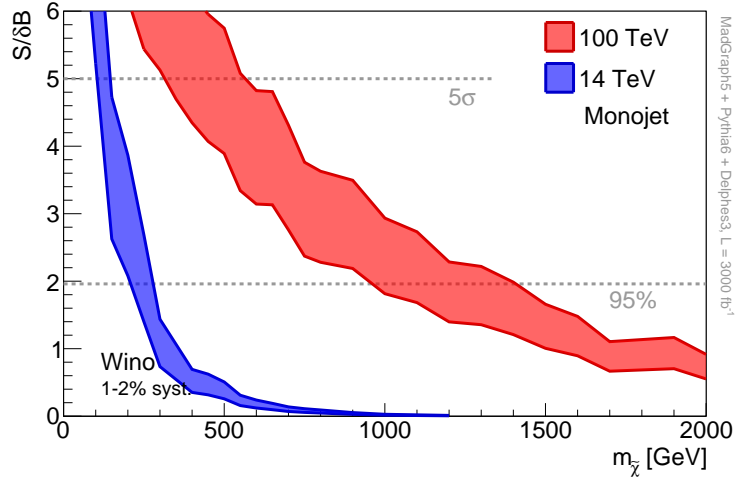


Figure 1: The mass reach in the pure wino scenario in the monojet channel with $\mathcal{L} = 3000 \text{ fb}^{-1}$ for the 14 TeV LHC (blue) and a 100 TeV proton-proton collider (red). The bands are generated by varying the background systematics between 1 – 2% and the signal systematic uncertainty is set to 10%.

For reference, ignoring all systematics, at 14 TeV winos could be excluded at $m_{\tilde{\chi}} \sim 530 \text{ GeV}$ and discovered at $m_{\tilde{\chi}} \sim 380 \text{ GeV}$. At 100 TeV the exclusion reach would be $m_{\tilde{\chi}} \sim 1.8 \text{ TeV}$ and the discovery reach would be $m_{\tilde{\chi}} \sim 1.0 \text{ TeV}$.

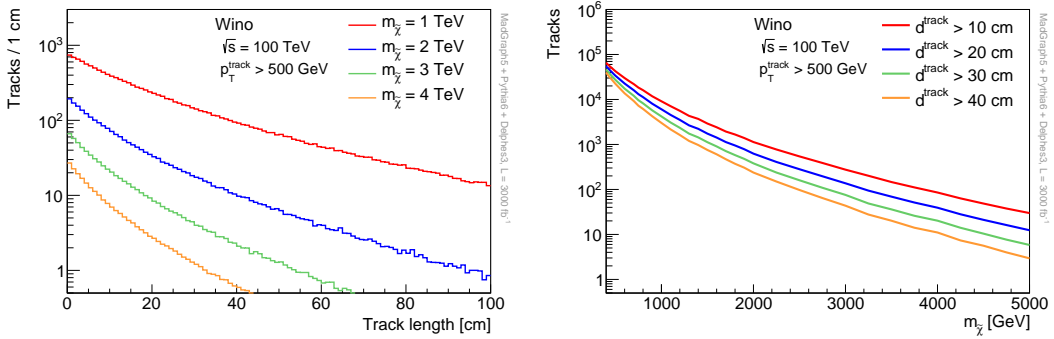


Figure 2: Chargino track distributions for the pure wino scenario showing the number of tracks for a given track length (left) and the number of tracks for a given wino mass (right). Only events passing the analysis cuts in App. A and containing at least one chargino track with $p_T > 500 \text{ GeV}$ are considered.

As mentioned, in the pure wino scenario, the mass splitting between the chargino and neutralino is generated by loop effects. The value of the splitting has been calculated at two-loops to be $\Delta = 164.6 \text{ MeV}$ in the large mass limit [83], though the mass splitting varies very

little with respect to wino mass. A mass splitting can also be generated by higher dimension operators. For the pure wino, the lowest operator that can split the charged and neutral states is dimension 7, so the splitting cited above is fairly model-independent. In our simulation we use the lifetime calculated at one-loop. At a collider the lifetime in the lab-frame also includes the velocity β and boost γ so that $d = \beta\gamma c\tau$. Notice that $\beta\gamma$ can be substantially larger at 100 TeV than at 14 TeV.

The distribution of chargino track lengths is shown in Fig. 2 (left). At ATLAS the disappearing track search is conducted using the tracker which has a high efficiency for selecting disappearing tracks starting at $d^{\text{track}} \sim 30$ cm. A detector with a similarly designed tracker would observe a handful of tracks for WIMPs as heavy as $m_{\tilde{\chi}} \sim 3$ TeV. Fig. 2 (right) shows directly the number of tracks for a given LSP mass for various requirements on the length of a track. While no upper limit on track length is enforced in Fig. 2, as the distribution is exponential the value of the upper limit, $d^{\text{track}} \sim 80$ cm for ATLAS [64], has a negligible impact⁴.

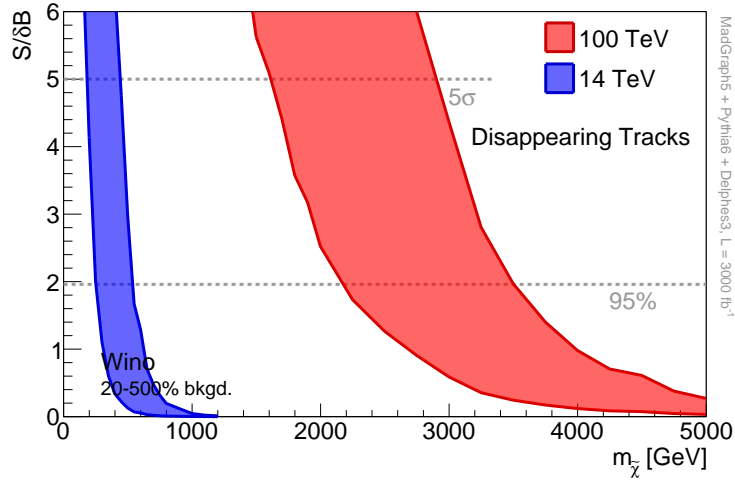


Figure 3: The mass reach in the pure wino scenario in the disappearing track channel with $\mathcal{L} = 3000 \text{ fb}^{-1}$ for the 14 TeV LHC (blue) and a 100 TeV proton-proton collider (red). The bands are generated by varying the background normalization between 20 – 500%. Only events passing the analysis cuts in App. A are considered.

Since the dominant background for a disappearing track search would be mismeasured low p_T tracks, it is not possible to accurately project the background in a yet-to-be-designed detector at a 100 TeV proton-proton collider. Nevertheless, Fig. 2 can serve as a rough guide. For example, one could require $d^{\text{track}} > 30$ cm and there be tens of signal events

⁴The pure wino scenario results in a chargino lifetime of $c\tau \sim 6$ cm in the bulk of the mass range. Even with the boost $d^{\text{track}} = \gamma\beta c\tau$, most charginos decay before reaching the end of the inner detector. However, if the chargino lifetime were modified such that $c\tau \sim d^{\text{tracker}}$, then the length of the tracker becomes a relevant parameter.

passing all cuts, which is roughly where the 8 TeV ATLAS limit is set. We choose to attempt a more systematic approach and naively extrapolate the dominant ATLAS background of mismeasured tracks. The ATLAS search selects events with one or two hard jets and large \cancel{E}_T where neither of the jets can be too close to the \cancel{E}_T direction. As this is the same criteria as the monojet search we estimate the background normalization to be set by the $Z(\nu\nu) + \text{jets}$ rate. Additional details on our scaling procedure are found in App. A. The results of the extrapolation are shown in Fig. 3 with $\gamma = 10\%$ and $\lambda = 20\%$. The band is generated by varying the background normalization up and down by a factor of 5.

The results are summarized in Table 1. In the monojet channel, we find that a 100 TeV collider extends the wino mass reach about 4–5 times that of the LHC entering the TeV mass range. A much more promising search, however, is the disappearing track search. Already at 8 TeV this channel has been shown to be more sensitive than a monojet search [64], and this continues to be the case at 100 TeV. Depending on the detector-backgrounds, this search has the potential to rule out (or perhaps discover) thermal winos.

channel	systematics/ normalization	14 TeV		100 TeV	
		95% limit	5σ discovery	95% limit	5σ discovery
monojet	1%	280 GeV	140 GeV	1.4 TeV	560 GeV
	2%	205 GeV	100 GeV	960 GeV	310 GeV
disappearing tracks	500%	250 GeV	180 GeV	2.1 TeV	1.6 TeV
	100%	385 GeV	295 GeV	2.9 TeV	2.2 TeV
	20%	535 GeV	440 GeV	3.5 TeV	2.9 TeV

Table 1: Mass reach for the pure wino scenario. For the monojet channel, the second column shows the systematic uncertainty on the background used, while the systematic uncertainty on the signal was 10%. For the disappearing tracks channel, the second column shows the background normalization. For this channel the background systematic uncertainty was 20% and the signal systematic uncertainty was 10%.

4 Pure Higgsino

Another interesting class of SUSY spectra are those that contain a higgsino as the LSP. Because of the connection between μ and fine-tuning, these spectra arise in natural SUSY [84, 85], as well as in split SUSY [86] and mini-split SUSY [71]. A thermal higgsino saturates the relic density for $m_{\tilde{\chi}} \sim 1$ TeV, which like the thermal wino, is inaccessible to the LHC. The spin-independent scattering cross-section has been calculated to be $\sigma_{\text{SI}} \lesssim 10^{-48} \text{ cm}^2$ which is near or below the neutrino coherent scattering floor [81, 82]. While a 100 TeV collider can come much closer to the thermal value, likely it is still not able to rule out this scenario.

The higgsino is a vector-like doublet which results in two neutralinos and one chargino at low energies. This opens up additional pair production channels relative to the pure wino

case, but all channels are still through an s -channel W^\pm or Z .

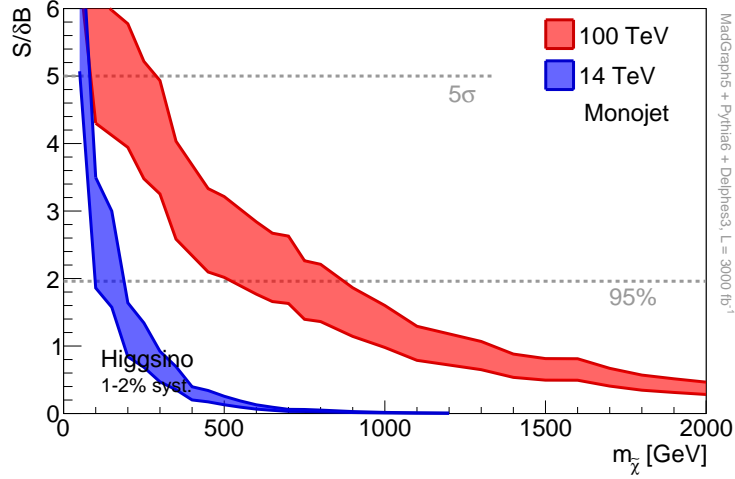


Figure 4: The mass reach in the pure higgsino scenario in the monojet channel with $\mathcal{L} = 3000 \text{ fb}^{-1}$ for the 14 TeV LHC (blue) and a 100 TeV proton-proton collider (red). The bands are generated by varying the background systematics between 1 – 2% and the signal systematic uncertainty is set to 10%.

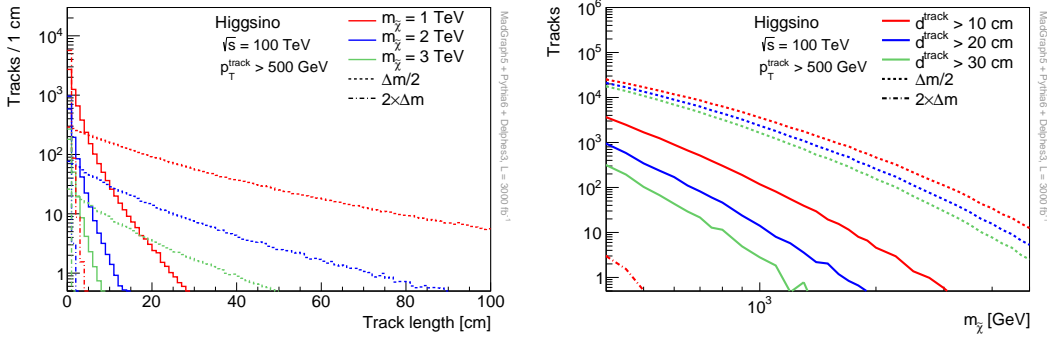


Figure 5: Chargino track distributions for the pure higgsino scenario showing the number of tracks for a given track length (left) and the number of tracks for a given higgsino mass (right). The dashed lines shows the same plots with a neutralino-chargino mass splitting half the standard value, and the dashed-dotted lines show the same plots with a neutralino-chargino mass splitting twice the standard value. Only events passing the analysis cuts in App. A and containing at least one chargino track with $p_T > 500 \text{ GeV}$ are considered.

Fig. 4 shows the mass reach in the monojet channel for the pure higgsino scenario. As in the wino case, there is a factor 4-5 enhancement in reach for the 100 TeV collider relative to the LHC. The reach is weaker than that for winos, mainly due to the reduction in production cross-section.

Without systematics one finds higgsinos could be excluded at $m_{\tilde{\chi}} \sim 410$ GeV and discovered at $m_{\tilde{\chi}} \sim 290$ GeV at 14 TeV, and excluded at $m_{\tilde{\chi}} \sim 1.2$ TeV and discovered at $m_{\tilde{\chi}} \sim 0.6$ TeV at 100 TeV.

It is also imaginable to do a disappearing track such for higgsinos. We note that, in comparison to the wino, it is more likely for heavier new particle states to alter the higgsino splitting as the lowest higher dimensional operator splitting the charged and neutral higgsinos is dimension 5. Therefore choosing a higgsino splitting has a larger degree of model dependence. In Fig. 5 (left) we show the distance of chargino tracks for the standard one-loop splittings, as well as for scenarios with twice the splitting and one half of the splitting. Fig. 5 (right) shows the corresponding plot for the number of tracks.

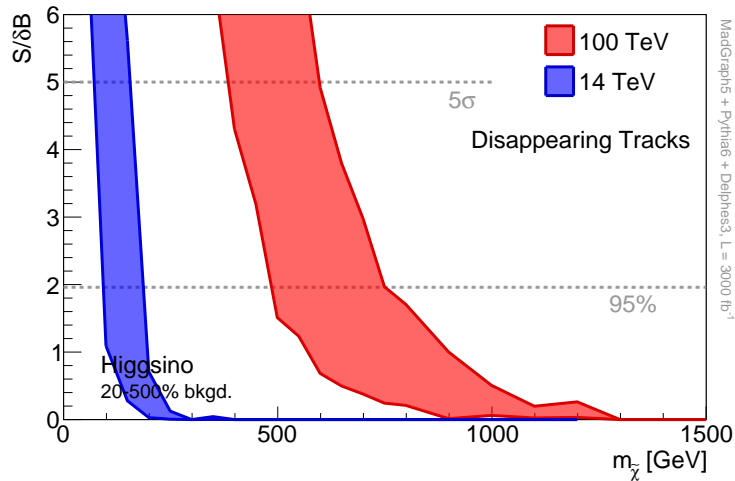


Figure 6: The mass reach in the pure higgsino scenario in the disappearing track channel with $\mathcal{L} = 3000 \text{ fb}^{-1}$ for the 14 TeV LHC (blue) and a 100 TeV proton-proton collider (red). The bands are generated by varying the background normalization between 20 – 500%. Only events passing the analysis cuts in App. A are considered.

Results are shown in Table 2. We find the monojet channel to reach $m_{\tilde{\chi}} \sim 870$ GeV. The disappearing track search is potentially a promising channel too, but depends sensitively on the chargino-neutralino mass splitting. The disappearing track with the canonical splitting is not as sensitive as the monojet search, but were the splitting to be decreased by a factor of two, the limits would be comparable to the reach for winos.

5 Mixed Spectra

In the previous two sections we studied the phenomenology of pure LSPs which feature nearly degenerate electroweakinos. In more general mixed scenarios, larger mass splittings between charginos and neutralinos can be generated. In this paper, we look at the compressed case

channel	systematics/ normalization	14 TeV		100 TeV	
		95% limit	5σ discovery	95% limit	5σ discovery
monojet	1%	185 GeV	80 GeV	870 GeV	285 GeV
	2%	95 GeV	50 GeV	580 GeV	80 GeV
disappearing tracks	20%	185 GeV	155 GeV	750 GeV	595 GeV
	100%	140 GeV	95 GeV	615 GeV	485 GeV
	500%	90 GeV	70 GeV	485 GeV	380 GeV

Table 2: Mass reach for the pure higgsino scenario. For the monojet channel, the second column shows the systematic uncertainty on the background used, while the systematic uncertainty on the signal was 10%. For the disappearing tracks channel, the second column shows the background normalization. For this channel the background systematic uncertainty was 20% and the signal systematic uncertainty was 10%.

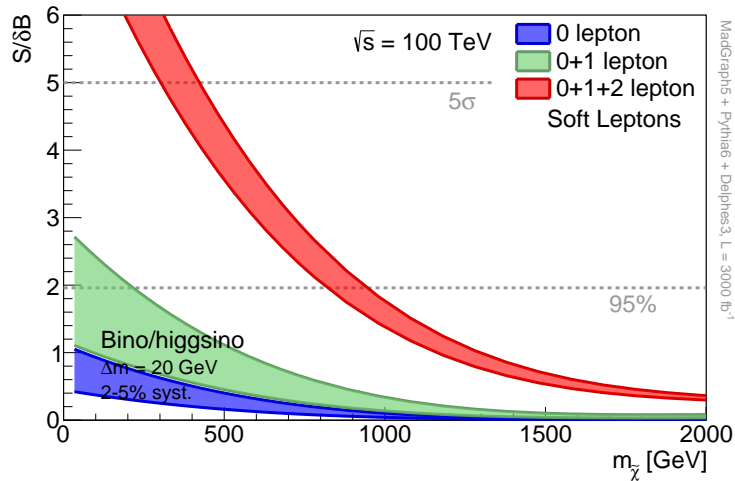


Figure 7: The mass reach in the mixed bino/higgsino ($\Delta = 20$ GeV) scenario in the soft lepton channel at 100 TeV with $\mathcal{L} = 3000 \text{ fb}^{-1}$ at 100 TeV looking for 0 leptons (blue), 0 or 1 leptons (green), and 0, 1, or 2 leptons (red). The bands are generated by varying the background systematics between 2 – 5% and the signal systematic uncertainty is set to 10%.

of $\Delta m = 20 - 30$ GeV, where the heavier charginos and neutralinos decay to the LSP via off-shell W 's and Z 's.

Unlike pure spectra, mixed spectra are known to be able to thermally saturate the relic density, for a range of masses. Examples include the well-tempered scenario [87] where $|M_1| \approx |M_2|$ or $|M_1| \approx |\mu|$ and the focus point region [88–92] where the LSP contains a non-trivial higgsino fraction. To thermally produce the correct relic abundance, one typically needs the LSP is be dominantly higgsino-like or wino-like and subdominantly bino-like.

As we have characterized spectra by their splitting between the LSP and lightest chargino,

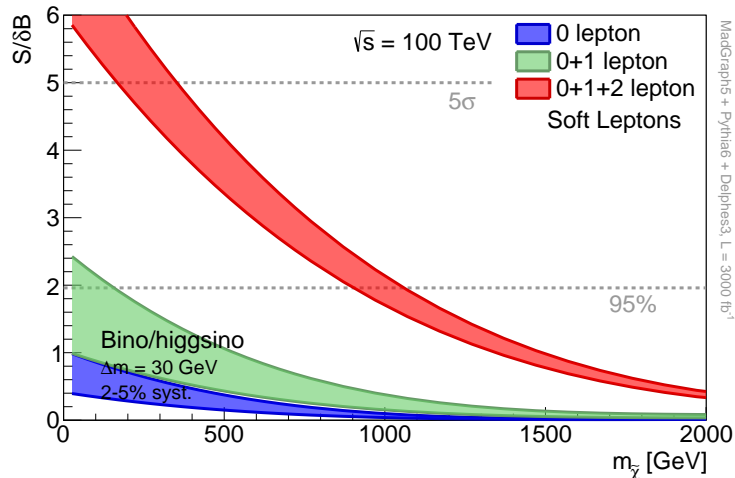


Figure 8: The mass reach in the mixed bino/higgsino ($\Delta = 30$ GeV) scenario in the soft lepton channel at 100 TeV with $\mathcal{L} = 3000$ fb $^{-1}$ at 100 TeV looking for 0 leptons (blue), 0 or 1 leptons (green), and 0, 1, or 2 leptons (red). The bands are generated by varying the background systematics between 2 – 5% and the signal systematic uncertainty is set to 10%.

these spectra typically have very small $\Delta m \gtrsim 0$. For very small Δm the best search tends to be the monojet search (covered in Sects. 3, 4, and 6). Because we elect to focus on the collider phenomenology of compressed spectra with soft leptons, we choose spectra with $\Delta m = 20 - 30$ GeV. While these spectra do not thermally saturate the relic density, they directly demonstrate the utility of soft lepton searches.

Relative to pure winos and higgsinos mixed dark matter can be strongly constrained by direct detection experiments which already and will continue to exclude large regions of parameter space [93–95].

In this paper we study the three following representative compressed spectra:

- (i) Bino/higgsino $\Delta = 20$ GeV: We scan over M_1 and set $\mu = -M_1 + 23$ GeV. The low energy states include three neutralinos and a chargino and the mass splitting is 20 GeV.
- (ii) Bino/higgsino $\Delta = 30$ GeV: We scan over M_1 and set $\mu = -M_1 - 2$ GeV. The low energy states include three neutralinos and a chargino and the mass splitting is 30 GeV.
- (iii) Bino/wino(/higgsino) $\Delta = 20$ GeV: We scan over M_1 and set $M_2 = M_1 + 34$ GeV and $\mu = M_1 + 120$ GeV. The low energy states include all four neutralinos and both charginos and the mass splitting is 20 GeV.

Figs. 7, 8, and 9 show the mass reach for scenarios (i), (ii), and (iii), respectively, in the soft lepton channel at 100 TeV⁵. Leptons are considered to be electrons with 10 GeV <

⁵In Figs. 7, 8, 9, and 10 the significances as a function of mass shown are fitted to a 4th order polynomial.

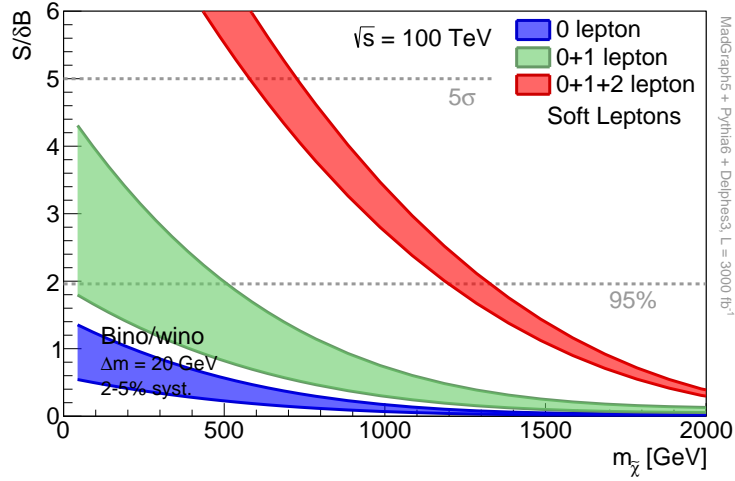


Figure 9: The mass reach in the mixed bino/wino(/higgsino) ($\Delta = 20$ GeV) scenario in the soft lepton channel at 100 TeV with $\mathcal{L} = 3000 \text{ fb}^{-1}$ at 100 TeV looking for 0 leptons (blue), 0 or 1 leptons (green), and 0, 1, or 2 leptons (red). The bands are generated by varying the background systematics between 2 – 5% and the signal systematic uncertainty is set to 10%.

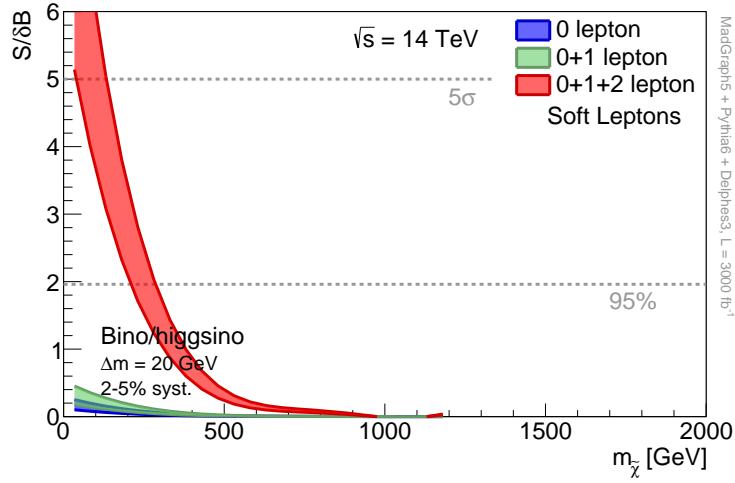


Figure 10: The mass reach in the mixed bino/higgsino ($\Delta = 20$ GeV) scenario in the soft lepton channel at 14 TeV with $\mathcal{L} = 3000 \text{ fb}^{-1}$ at 100 TeV looking for 0 leptons (blue), 0 or 1 leptons (green), and 0, 1, or 2 leptons (red). The bands are generated by varying the background systematics between 2 – 5% and the signal systematic uncertainty is set to 10%. The results for bino/higgsino ($\Delta = 30$ GeV) and bino/wino ($\Delta = 20$ GeV) are very similar.

As there are a relatively small number of leptons there are fluctuations in the bands due to statistics. The fit is not very sensitive to the polynomial used. Using a 3rd or 5th order polynomial instead only changes the

channel	LSP	Δm	bkgd. syst.	100 TeV	
				95% limit	5σ discovery
soft leptons	bino/higgsino	20 GeV	2%	940 GeV	420 GeV
			5%	820 GeV	300 GeV
	bino/higgsino	30 GeV	2%	1.0 TeV	350 GeV
			5%	0.9 TeV	165 GeV
	bino/wino	20 GeV	2%	1.3 TeV	725 GeV
			5%	1.2 TeV	575 GeV

Table 3: Mass reach for the mixed dark matter scenario. The systematic uncertainty on the signal was 10%. At 14 TeV the exclusion reach is $m_{\tilde{\chi}} \lesssim 200 - 280$ GeV (for 5 – 2%) and the discovery reach is $m_{\tilde{\chi}} \lesssim 30 - 130$ GeV (for 5 – 2%) for all three spectra.

$p_T < 30$ GeV or muons with $10 \text{ GeV} < p_T < 30$ GeV. In the plots the blue band shows the significance for the 0 lepton bin alone. Here we set $\lambda = 2 - 5\%$ due to possibly more sizable systematic uncertainties from identifying low p_T leptons and keep $\gamma = 10\%$. The green band shows the significance of the 0 and 1 lepton bins added in quadrature and the red band additionally includes the 2 lepton bin. Fig. 10 shows the bino/higgsino scenario for 14 TeV. We do not include the corresponding plots for the other mixed spectra as they yield very similar results.

Table 3 summarizes our results. We find in all cases the tagging of soft leptons plays a significant role in maximizing mass reach. In particular the 2-lepton bin noticeably drives the significance in all cases. This is because for the 0-lepton and 1-lepton bins the background is dominated by a single boson process. In the 2-lepton bin, the background is mostly a diboson process, which has a much smaller cross-section. The exclusion reach extends to $m_{\tilde{\chi}} \sim 1$ TeV in all cases and the discovery reaches several hundred GeV.

6 Coannihilating Spectra

In the discussion of thermally viable dark matter models another relevant set of models are those that include coannihilation. While bino LSPs alone oversaturate the relic abundance, if another particle is almost mass degenerate it can enhance the annihilation cross-section enough to produce the observed relic density [96]. In this section we explore four different spectra classified by the particles close in energy to the LSP: (i) gluinos, (ii) stops, (iii) squarks, and (iv) staus. While coannihilation with wino and higgsino LSPs are also possible, here we only consider a bino LSP.

The first spectrum we consider is gluino coannihilation. While such spectra do not arise in minimal supergravity, they can be realized in more general non-universal models. The phenomenology has been studied [97, 98] and the relic abundance has recently been calculated projections by a few GeV.

including Sommerfeld effects [99, 100]⁶. In the limit of the bino and gluino being mass degenerate, they find $m_{\tilde{\chi}} \sim 7.5$ TeV produces the correct relic density.

We set $m_{\tilde{g}} - m_{\tilde{\chi}} \approx 0.05m_{\tilde{\chi}}$ and decouple everything else, leaving one neutralino and the gluinos at low energies. Relic abundance calculations are very sensitive to the exact mass splitting used but collider processes much less sensitive. The signal consists of pair produced gluinos, which then decay to the LSP and other standard model particles which could be tagged. As the decays depend on details of the other SUSY particles we remain agnostic and assume the gluinos decay as $\tilde{g} \rightarrow \tilde{\chi}_1^0 + \text{undetected}$.

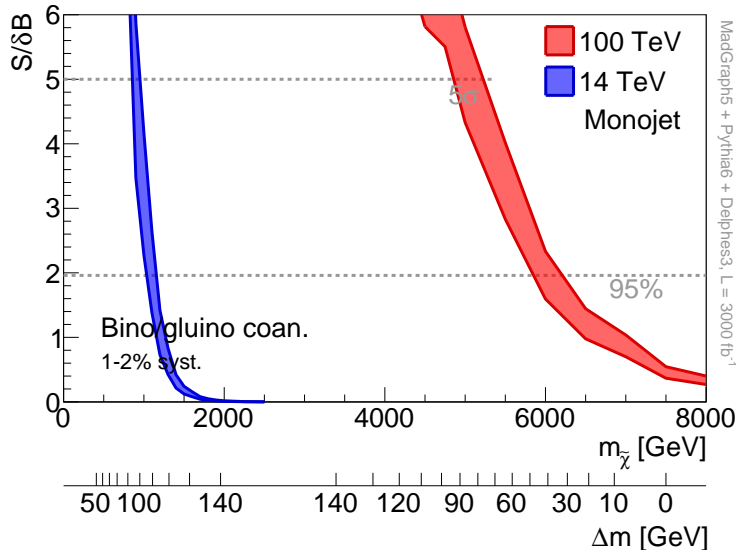


Figure 11: The mass reach in the gluino coannihilation scenario in the monojet channel with $\mathcal{L} = 3000 \text{ fb}^{-1}$ for the 14 TeV LHC (blue) and a 100 TeV proton-proton collider (red). The bands are generated by varying the background systematics between 1 – 2% and the signal systematic uncertainty is set to 10%. The lower x -axis displays the gluino-bino mass splitting Δm for a given bino mass which is required to saturate the relic density [99, 100]. A tick is placed every 10 GeV with the exception of the consecutive $\Delta m = 140$ GeV ticks.

Fig. 11 shows the mass reach applying the same monojet search as for the pure wino and higgsino. In this section we will continue to use $\gamma = 10\%$ and $\lambda = 1 - 2\%$. Given a bino mass and demanding that it saturate the relic density, one can find a gluino mass for which this is true. This defines the mass difference $\Delta m = m_{\tilde{g}} - m_{\tilde{\chi}}$ between the gluino and bino and has been calculated as a function of $m_{\tilde{\chi}}$ in [99, 100]. In Fig. 11, the x -axis shows the bino mass, while the lower x -axis denotes to the gluino-bino splitting required to saturate the relic density for the corresponding bino mass. As can be seen, a 100 TeV monojet search can rule

⁶There is a small difference in the mass splitting values found, $\Delta m \lesssim 10$ GeV, between [99] and [100] for gluino coannihilation. This difference is due to different choices in renormalization scales. In what follows we cite values calculated in [100].

out a bino LSP with $m_{\tilde{\chi}} \sim 6.2$ TeV and a gluino at $m_{\tilde{g}} \sim 6.23$ TeV (*i.e.* $\Delta m \sim 30$ GeV), but cannot exclude the case where $\Delta m = 0$ (corresponding to $m_{\tilde{\chi}} = m_{\tilde{g}} \sim 7.5$ TeV). If systematics are not considered the mass reach increases by ~ 350 GeV at 14 TeV and by ~ 250 GeV at 100 TeV.

The next coannihilator considered is the stop. As the mass of the stop is tied to fine-tuning, stop coannihilation appears in many models [101, 102] and has also been previously studied [103]. In our simulations we set $m_{\tilde{t}} - m_{\tilde{\chi}} \approx 0.05m_{\tilde{\chi}}$ and decouple everything else, leaving one neutralino and the right-handed stop at low energies.

The mass reach is shown in Fig. 12. The mass for a thermal bino is $m_{\tilde{\chi}} \sim 1.8$ TeV in the stop-degenerate limit. A 100 TeV collider can not only comfortably exclude this scenario, but also discover it, given sufficiently low systematics. Without systematics the mass reach increases by ~ 250 GeV at 14 TeV and by ~ 300 GeV at 100 TeV.

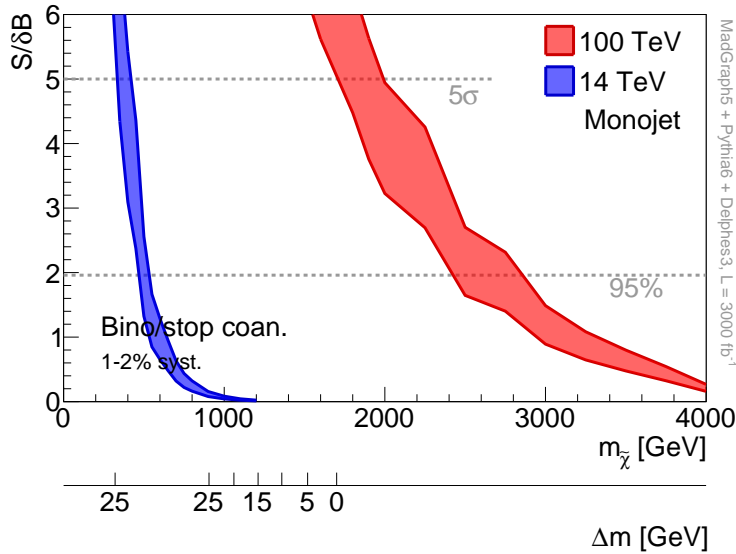


Figure 12: The mass reach in the stop coannihilation scenario in the monojet channel with $\mathcal{L} = 3000 \text{ fb}^{-1}$ for the 14 TeV LHC (blue) and a 100 TeV proton-proton collider (red). The bands are generated by varying the background systematics between 1 – 2% and the signal systematic uncertainty is set to 10%. The lower x -axis displays the stop-bino mass splitting Δm for a given bino mass which is required to satisfy the relic density [100]. A tick is placed every 5 GeV with the exception of the consecutive $\Delta m = 25$ GeV ticks.

Next we move onto squark coannihilation. For this spectrum we keep the left-handed scalar partners of the light quarks (\tilde{u}_L , \tilde{d}_L , \tilde{s}_L , and \tilde{c}_L) in the spectrum, while decoupling everything else. We set these in the same manner as in the other coannihilation spectra, $m_{\tilde{q}} - m_{\tilde{\chi}} \approx 0.05m_{\tilde{\chi}}$. Fig. 13 shows the monojet reach. As expected the significance is roughly four times larger than the stop coannihilation case. The exclusion reach extends to

$m_{\tilde{\chi}} \sim 4$ TeV and the discovery reach to $m_{\tilde{\chi}} \sim 3$ TeV. The mass reach goes up by ~ 300 GeV at 14 TeV and by ~ 500 GeV at 100 TeV if systematics are ignored.

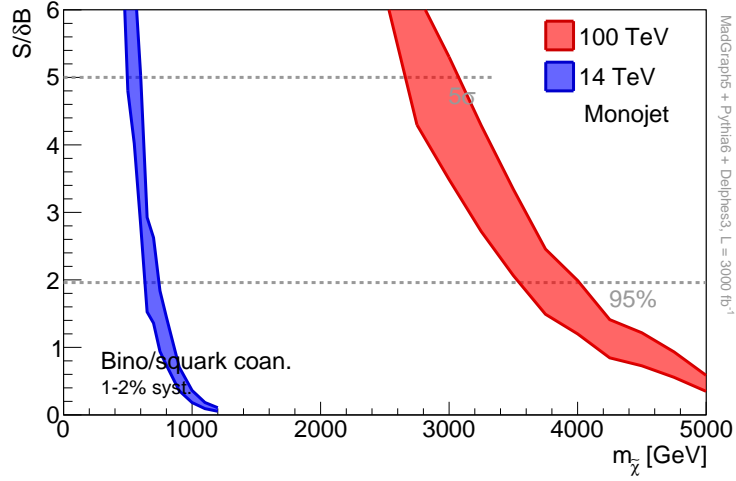


Figure 13: The mass reach in the squark coannihilation scenario in the monojet channel with $\mathcal{L} = 3000 \text{ fb}^{-1}$ for the 14 TeV LHC (blue) and a 100 TeV proton-proton collider (red). The bands are generated by varying the background systematics between 1 – 2% and the signal systematic uncertainty is set to 10%.

Lastly we studied the stau coannihilation scenario. These regions come up in constrained MSSM parameter scans, albeit with other particles at low energies [104]. Again, we set $m_{\tilde{\tau}} - m_{\tilde{\chi}} \approx 0.05m_{\tilde{\chi}}$, leaving a neutralino and the right-handed stau at low energies. The cross-section for stau pair production is suppressed by more than an order of magnitude relative to the strongly-interacting coannihilators and is too low for the monojet channel to have any sensitivity [105]. Projecting the reach in constrained MSSM stau coannihilation regions at 100 TeV would require a more detailed study involving other particles in the spectrum and different search channels.

The coannihilation results are summarized in Table 4. To recapitulate we find the exclusion reach for gluinos to be $m_{\tilde{\chi}} \sim 6.2$ TeV, for stops to be $m_{\tilde{\chi}} \sim 2.8$ TeV, and for squarks to be $m_{\tilde{\chi}} \sim 4.0$ TeV. The monojet search is not sensitive to the stau coannihilation scenario. The discovery prospects are also all in the multi-TeV range.

7 Conclusions

In this work we projected the 95% exclusion reach and the 5σ discovery reach of a 100 TeV proton-proton collider for neutralino dark matter. As SUSY already provides a variety of basic dark matter models we performed our study in the context of simplified SUSY models, but the results can be straightforwardly generalized. We implemented three collider searches,

channel	coannihilator	bkgd. syst.	14 TeV		100 TeV	
			95% limit	5σ discovery	95% limit	5σ discovery
monojet	gluino	1%	1.1 TeV	950 GeV	6.2 TeV	5.2 TeV
		2%	1.0 TeV	850 GeV	5.8 TeV	4.8 TeV
	stop	1%	530 GeV	420 GeV	2.8 TeV	2.1 TeV
		2%	470 GeV	330 GeV	2.4 TeV	1.7 TeV
	squark	1%	740 GeV	600 GeV	4.0 TeV	3.0 TeV
		2%	630 GeV	495 GeV	3.5 TeV	2.6 TeV
	stau	n/a	n/a	n/a	n/a	n/a

Table 4: Mass reach for the coannihilating dark matter scenario. The systematic uncertainty on the signal was 10%.

all of which relied on the basic signal of tagging one or more initial state radiation (ISR) jets and summarized in Fig. 14.

The first spectrum studied was pure wino dark matter. Recently, wino dark matter has received some attention based on the potential to exclude or discover it with indirect detection experiments. Unfortunately, the LHC is only able to probe the several hundred GeV range, which is neither near the thermally-saturating wino mass, nor high enough to close the available mass window from the low end (given a pessimistic dark matter halo profile). A 100 TeV collider, in contrast, can exclude as high as $m_{\tilde{\chi}} \sim 1.4$ TeV in the monojet channel, or even $m_{\tilde{\chi}} \sim 3$ TeV given a naive extrapolation of a disappearing track search. In light both of 8 TeV LHC results and this study, it is clear that the disappearing track (and displaced vertices and charged massive particle) search will play an exigent role in continuing to carve away at wino parameter space.

Higgsino dark matter was next to be looked at and was found to receive similar enhancements in mass reach in going from the LHC to a 100 TeV collider as wino dark matter. The higgsino cross-section, however, is lower than that of the wino, which is reflected in a lower exclusion and discovery reach. Respectively these reaches were found to be $m_{\tilde{\chi}} \sim 870$ GeV and $m_{\tilde{\chi}} \sim 285$ GeV. The chargino-neutralino mass splitting for higgsinos is parametrically larger than the wino mass splitting leading to short chargino track length and a less sensitive disappearing track search. The monojet or disappearing track searches alone are not likely to quite reach the thermal higgsino mass. One direction of future work would be to examine combining several searches to reach the thermal higgsino mass or augment the spectrum with additional particles to open up new search channels.

The next spectra were several cases of mixed dark matter with a compressed spectrum of $\Delta m = 20 - 30$ GeV. In these cases the most applicable search was looking for soft leptons in association with the hard ISR jet(s). The exclusion reach was found to be $m_{\tilde{\chi}} \sim 1$ TeV,

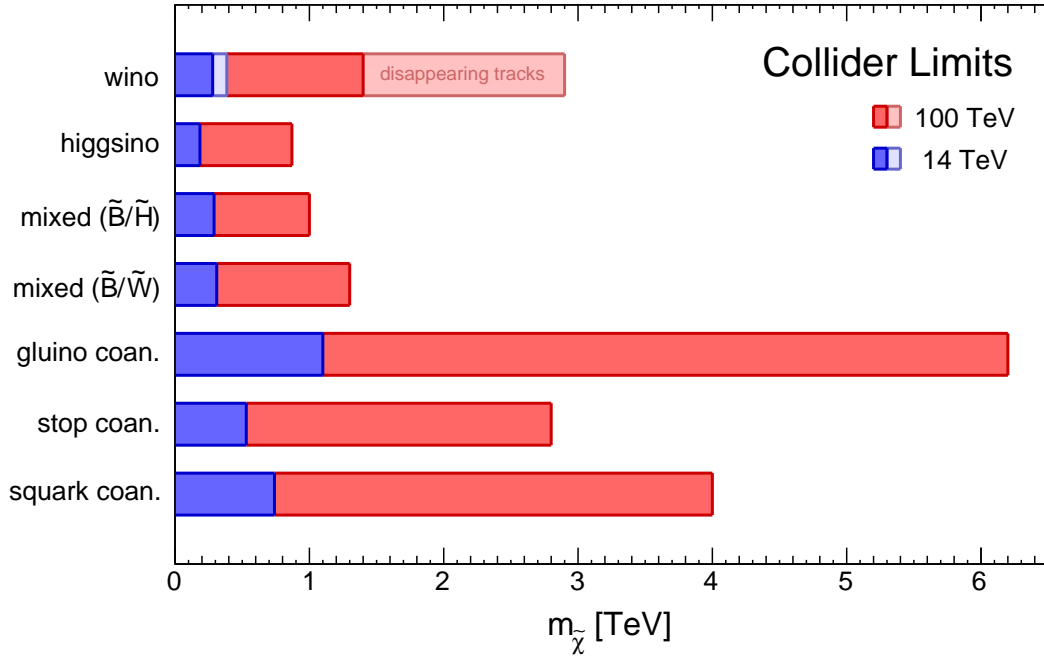


Figure 14: Summary of collider reach for neutralino dark matter.

while the discovery reach ranged from 350 – 700 GeV. Mixed dark matter parameter space already receives strong constraints from direct detection and a more thorough study on the impact of collider searches on this parameter space would be worthwhile.

Finally bino dark matter was studied, bringing various coannihilators into the spectrum to avoid overclosing the universe. These scenarios utilized the monojet search to project reach. The stop coannihilation exclusion reach was found to be $m_{\tilde{\chi}} \sim 2.8$ TeV and the discovery reach to be $m_{\tilde{\chi}} \sim 2.1$ TeV. As the thermally-saturating bino mass in this case is $m_{\tilde{\chi}} \sim 1.8$ TeV (and $m_{\tilde{t}} \sim 1.8$ TeV), dark matter can be either excluded or discovered in this channel. The gluino coannihilation, on the other hand, was found to only reach the thermal bino mass for a splitting of $\Delta m = 30$ GeV, corresponding to $m_{\tilde{\chi}} \sim 6.2$ TeV and $m_{\tilde{g}} \sim 6.23$ TeV, so the thermal parameter space is not entirely closed. Finally squark coannihilation can be excluded up to $m_{\tilde{\chi}} \sim 4.0$ TeV and stau coannihilation cannot be probed in the monojet channel.

In addition to the aforementioned interplay with mixed dark matter and neutralino blindspots, useful future work would be to look at how adding in more search channels can improve the dark matter collider reach. Such searches would include monophoton searches, razor searches, vector boson fusions searches, and multilepton searches. Another principal direction to extend these studies would be to look at the impact of bringing down other particles into the low energy spectrum.

In conclusion, we have shown that while the 14 TeV LHC can probe dark matter of several hundred GeV, a 100 TeV proton-proton collider could foray directly into the multi-TeV range. As this is precisely the range where thermally-saturating neutralino dark matter lives, a 100 TeV collider has great potential for discovering WIMP dark matter. Were a discovery to be made in the near future, a 100 TeV collider will be a vital tool for understanding the nature of dark matter.

Acknowledgments

The authors would like to thank Nima Arkani-Hamed, Alan Barr, Philip Harris, Shigeki Matsumoto, Steven Schramm, Pedro Schwaller, and Alessandro Strumia, as well as the participants of BSM Opportunities at 100 TeV Workshop for useful discussions.

ML is supported by NSERC of Canada and LTW is supported by DOE grant DE-SC0003930. Computations for this paper were performed on the Hypnotoad cluster supported by PSD Computing at the University of Chicago.

A Analysis Details

Monojet

Our monojet analysis closely follows the 8 TeV CMS monojet analysis [43]. To validate our background monte carlo and analysis we duplicated the CMS monojet cuts at 8 TeV and found good agreement across the cut flow. The only discrepancy present in our simulation was a slightly increased lepton efficiency due to the settings of the Snowmass detector card we used.

The 8 TeV analysis proceeds as:

- Require a hard central jet $p_T(j_1) > 110$ GeV, $|\eta(j_1)| < 2.4$.
- A second jet, defined as $p_T(j_2) > 30$ GeV, $|\eta(j_2)| < 4.5$, is permitted, but any additional jets are vetoed $n_{\text{jet}} \leq 2$.
- If there is a second jet it cannot be back-to-back with the hardest jet $\Delta\phi(j_1, j_2) < 2.5$.
- Identified leptons are vetoed. To be identified, electrons need to have $p_T(e) > 10$ GeV and $|\eta(e)| < 2.5$, muons need to have $p_T(\mu) > 10$ GeV and $|\eta(\mu)| < 2.1$ and reconstructed hadronic taus need to have $p_T(\tau) > 20$ GeV and $|\eta(\tau)| < 2.3$.
- The signal regions are defined in overlapping \cancel{E}_T bins: > 250 GeV, > 300 GeV, > 350 GeV, > 400 GeV, > 450 GeV, > 500 GeV, and > 550 GeV. The bin with the highest expected significance is used to set the limit.

At 14 TeV and 100 TeV the cuts were adjusted as shown in Tables 5 and 6.

Cut	8 TeV	14 TeV	100 TeV
$p_T(j_1), \eta(j_1)$	110 GeV, 2.4	300 GeV, 2.4	1200 GeV, 2.4
$p_T(j_2), \eta(j_2)$	30 GeV, 4.5	30 – 120 GeV, 4.5	100 – 400 GeV, 4.5
n_{jet}	2	2	2
$\Delta\phi(j_1, j_2)$	2.5	2.5	2.5
$p_T(e), \eta(e)$	10 GeV, 2.5	20 GeV, 2.5	20 GeV, 2.5
$p_T(\mu), \eta(\mu)$	10 GeV, 2.1	20 GeV, 2.1	20 GeV, 2.1
$p_T(\tau), \eta(\tau)$	20 GeV, 2.3	30 GeV, 2.3	40 GeV, 2.3
\cancel{E}_T	250 – 550 GeV	350 – 1000 GeV	2 – 5 TeV

Table 5: Cuts used in monojet analysis. For $p_T(j_2)$ and \cancel{E}_T the range represents the values scanned over, where the values used for each spectra are shown in Table 6.

\sqrt{s}	Cut	Wino	Higgsino	Gluino coan.	Stop coan.	Squark coan.	Stau coan.
14 TeV	\cancel{E}_T	650 GeV	650 GeV	750 GeV	650 GeV	650 GeV	650 GeV
	$p_T(j_2)$	30 GeV	30 GeV	120 GeV	120 GeV	120 GeV	120 GeV
100 TeV	\cancel{E}_T	3.5 TeV	3.5 TeV	4.0 TeV	3.5 TeV	3.5 TeV	3.5 TeV
	$p_T(j_2)$	300 GeV	250 GeV	400 GeV	400 GeV	400 GeV	400 GeV

Table 6: \cancel{E}_T and $p_T(j_2)$ cuts used in the monojet analysis for each spectra. Table 5 shows the other cuts used.

In light of the higher rates and luminosity for the 14 TeV and 100 TeV we also explored if the significance can be improved by applying additional cuts. We found that allowing for a third jet and making cuts on the various distances between jets did not help because the signal and backgrounds have very similar kinematics. The distributions are not identical, however, and it is possible that a clever analysis, like razor [106–108] for instance, could still yield a small improvement.

Soft Leptons

The soft lepton analysis is similar to the monojet analysis with the exception of how leptons are treated. Events are binned according to whether they contain 0, 1, or 2 leptons where a lepton is defined as an electron with $10 \text{ GeV} < p_T(e) < 30 \text{ GeV}$ or a muon with $10 \text{ GeV} < p_T(\mu) < 30 \text{ GeV}$. Hadronic taus are not tagged. The bins are assumed to be uncorrelated and their significances are added in quadrature.

Disappearing Tracks

For signal events we replicate the analysis in the 8 TeV ATLAS analysis [64], which applies the following cuts

- Require a hard jet $p_T(j_1) > 90 \text{ GeV}$.

Cut	100 TeV	14 TeV
$p_T(j_1), \eta(j_1)$	1200 GeV, 2.4	300 GeV, 2.4
$p_T(j_2), \eta(j_2)$	300 GeV, 4.5	30 GeV, 4.5
n_{jet}	2	2
$\Delta\phi(j_1, j_2)$	2.5	2.5
$p_T(e), \eta(e)$	$\in (10 \text{ GeV}, 30 \text{ GeV}), 2.5$	$\in (10 \text{ GeV}, 30 \text{ GeV}), 2.5$
$p_T(\mu), \eta(\mu)$	$\in (10 \text{ GeV}, 30 \text{ GeV}), 2.1$	$\in (10 \text{ GeV}, 30 \text{ GeV}), 2.1$
\cancel{E}_T	1250 GeV	350 GeV

Table 7: Cuts used in soft lepton analysis.

Cut	8 TeV	14 TeV	100 TeV
\cancel{E}_T	90 GeV	130 GeV	975 GeV
$p_T(j_1)$	90 GeV	130 GeV	975 GeV
$p_T(j_2)$	45 GeV	70 GeV	500 GeV
$\Delta\phi_{\text{min}}(j, \cancel{E}_T)$	1.5	1.5	1.5
η^{track}	$\in (0.1, 1.9)$	$\in (0.1, 1.9)$	$\in (0.1, 1.9)$
p_T^{track}	75 – 200 GeV	250 GeV	1.5 TeV

Table 8: Cuts used in disappearing track analysis.

- Require that $\cancel{E}_T > 90 \text{ GeV}$.
- If there are any other jets with $p_T(j_2) > 45 \text{ GeV}$, the hardest of these is considered the second jet.
- Compute the azimuthal separation, $\Delta\phi(j, \cancel{E}_T)$, between the missing energy and the hardest jet. If there is a second jet and its azimuthal separation from the missing energy is smaller, use that instead. Only keep events where $\Delta\phi_{\text{min}}(j, \cancel{E}_T) > 1.5$.
- There must be at least chargino track that is isolated and satisfies a track selection criteria and $0.1 < |\eta^{\text{track}}| < 1.9$.
- Signal regions are defined by a p_T cut on the chargino track. The bins are $p_T^{\text{track}} > 75 \text{ GeV}$, $p_T^{\text{track}} > 100 \text{ GeV}$, $p_T^{\text{track}} > 150 \text{ GeV}$, and $p_T^{\text{track}} > 200 \text{ GeV}$.

We implement the isolation cut by rejecting events with jets within $\Delta R < 0.4$ of the chargino track, where $\Delta R = \sqrt{(\Delta\eta)^2 + (\Delta\phi)^2}$. To mock up the good track selection we assume the efficiency factors as $\epsilon_{\text{track}} = \epsilon_{\text{det}} \times \epsilon_{\text{tracker}}$, where we assume $\epsilon_{\text{tracker}}$ is 100% for tracks with a length $30 \text{ cm} < d^{\text{track}} < 80 \text{ GeV}$ and 0% otherwise and that ϵ_{det} is flat with respect to p_T^{track} and η^{track} . We derive ϵ_{det} by matching our event count from monte carlo to the event count from [64].

In the ATLAS 8 TeV study, in the signal region the dominant background is from mis-measured tracks and found to fit to a power law

$$\frac{d\sigma}{dp_T} = \sigma_0 p_T^{-a}, \quad (\text{A.1})$$

where p_T is measured in GeV, σ_0 is the normalization, and $a = 1.78 \pm 0.05$. We extrapolate this by assuming that the majority of events passing the cuts in Table 8 are $Z(\nu\nu)$ +jets events. Under this assumption we scale the normalization according to the $Z(\nu\nu)$ +jets cross-section after the cuts in Table 8 and make the appropriate p_T cut. We find σ_0 by matching to the ATLAS result.

B Extrapolating Systematics

While it is impossible to project the systematic uncertainties for a not-yet-designed detector, many of the systematics are generic features of detector technology. For completeness we list the dominant contributions to the various analyses here. More detailed discussions are found in the appropriate experimental analyses [40–43, 64].

The dominant contributions to systematics are

- *Jet uncertainties*: the jet energy scale and jet energy resolution determine how well jets, and consequently \cancel{E}_T , can be measured. These reduce at higher luminosity as the detector becomes better understood. Calorimeter measurements should be better at higher energies so these will likely naturally decrease at a 100 TeV collider (assuming a deep enough calorimeter).
- *Monte carlo uncertainties*: backgrounds are typically computed by counting events in a control region and extrapolating to the signal region using ratios computed by monte carlo generators. The uncertainty on the backgrounds is determined by the number of events in the control regions and the monte carlo extrapolation. At high luminosity the control regions will contain more events reducing the statistical uncertainties. This will also help create control regions for subdominant backgrounds, *e.g.* $t\bar{t}$ and diboson, which are currently determined entirely from monte carlo. These backgrounds can have uncertainties as large as $\sim 100\%$.

Additionally, monte carlo modeling can be improved by including higher-order perturbative corrections. Given the recent advancements in monte carlo technology (see [109] and references therein) it may be reasonable to expect similar leaps by the time a 100 TeV collider is built.

- *Lepton uncertainties*: precise measurements of lepton momenta are not only important in the soft lepton analysis, but also in the monojet and disappearing track analyses. While leptons are vetoed in the latter two searches, they are important in defining the control regions. Unfortunately muons are detected via tracking which degrades at

higher p_T . It will be important for the detectors at 100 TeV to maintain the ability to measure energetic muons to a reasonable precision.

References

- [1] G. Bertone, D. Hooper, and J. Silk, *Particle dark matter: Evidence, candidates and constraints*, *Phys.Rept.* **405** (2005) 279–390, [[hep-ph/0404175](#)].
- [2] G. Jungman, M. Kamionkowski, and K. Griest, *Supersymmetric dark matter*, *Phys.Rept.* **267** (1996) 195–373, [[hep-ph/9506380](#)].
- [3] S. P. Martin, *A Supersymmetry primer*, [hep-ph/9709356](#).
- [4] LHC New Physics Working Group, D. Alves et al., *Simplified Models for LHC New Physics Searches*, *J.Phys.* **G39** (2012) 105005, [[arXiv:1105.2838](#)].
- [5] T. Cohen, T. Golling, M. Hance, A. Henrichs, K. Howe, et al., *SUSY Simplified Models at 14, 33, and 100 TeV Proton Colliders*, [arXiv:1311.6480](#).
- [6] A. Fowlie and M. Raidal, *Prospects for constrained supersymmetry at $\sqrt{s} = 33$ TeV and $\sqrt{s} = 100$ TeV proton-proton super-colliders*, [arXiv:1402.5419](#).
- [7] J. D. Wells, *Implications of supersymmetry breaking with a little hierarchy between gauginos and scalars*, [hep-ph/0306127](#).
- [8] N. Arkani-Hamed and S. Dimopoulos, *Supersymmetric unification without low energy supersymmetry and signatures for fine-tuning at the LHC*, *JHEP* **0506** (2005) 073, [[hep-th/0405159](#)].
- [9] G. Giudice and A. Romanino, *Split supersymmetry*, *Nucl.Phys.* **B699** (2004) 65–89, [[hep-ph/0406088](#)].
- [10] M. Beltran, D. Hooper, E. W. Kolb, Z. A. Krusberg, and T. M. Tait, *Maverick dark matter at colliders*, *JHEP* **1009** (2010) 037, [[arXiv:1002.4137](#)].
- [11] P. J. Fox, R. Harnik, J. Kopp, and Y. Tsai, *Missing Energy Signatures of Dark Matter at the LHC*, *Phys.Rev.* **D85** (2012) 056011, [[arXiv:1109.4398](#)].
- [12] Y. Gershtein, F. Petriello, S. Quackenbush, and K. M. Zurek, *Discovering hidden sectors with mono-photon Z' searches*, *Phys.Rev.* **D78** (2008) 095002, [[arXiv:0809.2849](#)].
- [13] P. J. Fox, R. Harnik, J. Kopp, and Y. Tsai, *LEP Shines Light on Dark Matter*, *Phys.Rev.* **D84** (2011) 014028, [[arXiv:1103.0240](#)].
- [14] Y. Bai and T. M. Tait, *Searches with Mono-Leptons*, *Phys.Lett.* **B723** (2013) 384–387, [[arXiv:1208.4361](#)].
- [15] F. J. Petriello, S. Quackenbush, and K. M. Zurek, *The Invisible Z' at the CERN LHC*, *Phys.Rev.* **D77** (2008) 115020, [[arXiv:0803.4005](#)].
- [16] L. M. Carpenter, A. Nelson, C. Shimmin, T. M. Tait, and D. Whiteson, *Collider searches for dark matter in events with a Z boson and missing energy*, *Phys.Rev.* **D87** (2013), no. 7 074005, [[arXiv:1212.3352](#)].
- [17] A. A. Petrov and W. Shepherd, *Searching for dark matter at LHC with Mono-Higgs production*, *Phys.Lett.* **B730** (2014) 178–183, [[arXiv:1311.1511](#)].

- [18] L. Carpenter, A. DiFranzo, M. Mulhearn, C. Shimmin, S. Tulin, et al., *Mono-Higgs: a new collider probe of dark matter*, [arXiv:1312.2592](#).
- [19] A. Berlin, T. Lin, and L.-T. Wang, *Mono-Higgs Detection of Dark Matter at the LHC*, [arXiv:1402.7074](#).
- [20] P. Schwaller and J. Zurita, *Compressed electroweakino spectra at the LHC*, [arXiv:1312.7350](#).
- [21] C. Han, A. Kobakhidze, N. Liu, A. Saavedra, L. Wu, et al., *Probing Light Higgsinos in Natural SUSY from Monojet Signals at the LHC*, *JHEP* **1402** (2014) 049, [[arXiv:1310.4274](#)].
- [22] B. Bhattacharjee, A. Choudhury, K. Ghosh, and S. Poddar, *Compressed SUSY at 14 TeV LHC*, *Phys.Rev.* **D89** (2014) 037702, [[arXiv:1308.1526](#)].
- [23] H. Baer, A. Mustafayev, and X. Tata, *Monojets and mono-photons from light higgsino pair production at LHC14*, [arXiv:1401.1162](#).
- [24] Z. Han, G. D. Kribs, A. Martin, and A. Menon, *Hunting Quasi-Degenerate Higgsinos*, [arXiv:1401.1235](#).
- [25] N. Zhou, D. Berge, L. Wang, D. Whiteson, and T. Tait, *Sensitivity of future collider facilities to WIMP pair production via effective operators and light mediators*, [arXiv:1307.5327](#).
- [26] A. Djouadi, J.-L. Kneur, and G. Moultaka, *SuSpect: A Fortran code for the supersymmetric and Higgs particle spectrum in the MSSM*, *Comput.Phys.Commun.* **176** (2007) 426–455, [[hep-ph/0211331](#)].
- [27] J. Alwall, M. Herquet, F. Maltoni, O. Mattelaer, and T. Stelzer, *MadGraph 5 : Going Beyond*, *JHEP* **1106** (2011) 128, [[arXiv:1106.0522](#)].
- [28] T. Sjostrand, S. Mrenna, and P. Z. Skands, *PYTHIA 6.4 Physics and Manual*, *JHEP* **0605** (2006) 026, [[hep-ph/0603175](#)].
- [29] DELPHES 3, J. de Favereau et al., *DELPHES 3, A modular framework for fast simulation of a generic collider experiment*, *JHEP* **1402** (2014) 057, [[arXiv:1307.6346](#)].
- [30] J. Anderson, A. Avetisyan, R. Brock, S. Chekanov, T. Cohen, et al., *Snowmass Energy Frontier Simulations*, [arXiv:1309.1057](#).
- [31] A. Avetisyan, S. Bhattacharya, M. Narain, S. Padhi, J. Hirschauer, et al., *Snowmass Energy Frontier Simulations using the Open Science Grid (A Snowmass 2013 whitepaper)*, [arXiv:1308.0843](#).
- [32] A. Avetisyan, J. M. Campbell, T. Cohen, N. Dhingra, J. Hirschauer, et al., *Methods and Results for Standard Model Event Generation at $\sqrt{s} = 14$ TeV, 33 TeV and 100 TeV Proton Colliders (A Snowmass Whitepaper)*, [arXiv:1308.1636](#).
- [33] M. Cacciari, G. P. Salam, and G. Soyez, *The Anti- $k(t)$ jet clustering algorithm*, *JHEP* **0804** (2008) 063, [[arXiv:0802.1189](#)].
- [34] M. Cacciari, G. P. Salam, and G. Soyez, *FastJet User Manual*, *Eur.Phys.J.* **C72** (2012) 1896, [[arXiv:1111.6097](#)].
- [35] W. Beenakker, M. Klasen, M. Kramer, T. Plehn, M. Spira, et al., *The Production of charginos / neutralinos and sleptons at hadron colliders*, *Phys.Rev.Lett.* **83** (1999) 3780–3783, [[hep-ph/9906298](#)].

- [36] G. Cullen, N. Greiner, and G. Heinrich, *Susy-QCD corrections to neutralino pair production in association with a jet*, *Eur.Phys.J.* **C73** (2013) 2388, [[arXiv:1212.5154](#)].
- [37] D0 Collaboration, V. Abazov et al., *Search for large extra dimensions in the monojet + missing E_T channel at $D\bar{O}$* , *Phys.Rev.Lett.* **90** (2003) 251802, [[hep-ex/0302014](#)].
- [38] CDF Collaboration, T. Aaltonen et al., *Search for large extra dimensions in final states containing one photon or jet and large missing transverse energy produced in $p\bar{p}$ collisions at $\sqrt{s} = 1.96$ -TeV*, *Phys.Rev.Lett.* **101** (2008) 181602, [[arXiv:0807.3132](#)].
- [39] D0 Collaboration, V. Abazov et al., *Search for large extra dimensions via single photon plus missing energy final states at $\sqrt{s} = 1.96$ -TeV*, *Phys.Rev.Lett.* **101** (2008) 011601, [[arXiv:0803.2137](#)].
- [40] ATLAS Collaboration, G. Aad et al., *Search for dark matter candidates and large extra dimensions in events with a jet and missing transverse momentum with the ATLAS detector*, *JHEP* **1304** (2013) 075, [[arXiv:1210.4491](#)].
- [41] CMS Collaboration, S. Chatrchyan et al., *Search for dark matter and large extra dimensions in monojet events in pp collisions at $\sqrt{s} = 7$ TeV*, *JHEP* **1209** (2012) 094, [[arXiv:1206.5663](#)].
- [42] ATLAS Collaboration, *Search for New Phenomena in Monojet plus Missing Transverse Momentum Final States using 10fb-1 of pp Collisions at $\sqrt{s}=8$ TeV with the ATLAS detector at the LHC*, ATLAS-CONF-2012-147, ATLAS-COM-CONF-2012-190.
- [43] CMS Collaboration, *Search for new physics in monojet events in pp collisions at $\sqrt{s} = 8$ TeV*, CMS-PAS-EXO-12-048.
- [44] H. An, R. Huo, and L.-T. Wang, *Searching for Low Mass Dark Portal at the LHC*, *Phys.Dark Univ.* **2** (2013) 50–57, [[arXiv:1212.2221](#)].
- [45] H. An, X. Ji, and L.-T. Wang, *Light Dark Matter and Z' Dark Force at Colliders*, *JHEP* **1207** (2012) 182, [[arXiv:1202.2894](#)].
- [46] H. An, L.-T. Wang, and H. Zhang, *Dark matter with t -channel mediator: a simple step beyond contact interaction*, [arXiv:1308.0592](#).
- [47] CMS Collaboration, *Search for electroweak production of charginos, neutralinos, and sleptons using leptonic final states in pp collisions at 8 TeV*, CMS-PAS-SUS-13-006.
- [48] CMS Collaboration, *A search for anomalous production of events with three or more leptons using 19.5/fb of $\sqrt{s}=8$ TeV LHC data*, CMS-PAS-SUS-13-002.
- [49] CMS Collaboration, *Search for supersymmetry in pp collisions at $\sqrt{s} = 8$ TeV in events with three leptons and at least one b -tagged jet*, CMS-PAS-SUS-13-008.
- [50] ATLAS Collaboration, G. Aad et al., *Search for direct production of charginos and neutralinos in events with three leptons and missing transverse momentum in $\sqrt{s} = 8$ TeV pp collisions with the ATLAS detector*, [arXiv:1402.7029](#).
- [51] ATLAS Collaboration, G. Aad et al., *Search for direct production of charginos, neutralinos and sleptons in final states with two leptons and missing transverse momentum in pp collisions at $\sqrt{s} = 8$ TeV with the ATLAS detector*, [arXiv:1403.5294](#).
- [52] G. F. Giudice, T. Han, K. Wang, and L.-T. Wang, *Nearly Degenerate Gauginos and Dark Matter at the LHC*, *Phys.Rev.* **D81** (2010) 115011, [[arXiv:1004.4902](#)].

- [53] S. Gori, S. Jung, and L.-T. Wang, *Cornering electroweakinos at the LHC*, [arXiv:1307.5952](#).
- [54] S. D. Thomas and J. D. Wells, *Phenomenology of Massive Vectorlike Doublet Leptons*, *Phys.Rev.Lett.* **81** (1998) 34–37, [[hep-ph/9804359](#)].
- [55] M. Cirelli, N. Fornengo, and A. Strumia, *Minimal dark matter*, *Nucl.Phys.* **B753** (2006) 178–194, [[hep-ph/0512090](#)].
- [56] J. L. Feng and M. J. Strassler, *Determination of fundamental supersymmetry parameters from chargino production at LEP-2*, *Phys.Rev.* **D51** (1995) 4661–4694, [[hep-ph/9408359](#)].
- [57] J. L. Feng and M. J. Strassler, *Measuring SUSY parameters at LEP-2 using chargino production and decay*, *Phys.Rev.* **D55** (1997) 1326–1342, [[hep-ph/9606477](#)].
- [58] J. L. Feng, T. Moroi, L. Randall, M. Strassler, and S.-f. Su, *Discovering supersymmetry at the Tevatron in wino LSP scenarios*, *Phys.Rev.Lett.* **83** (1999) 1731–1734, [[hep-ph/9904250](#)].
- [59] J. F. Gunion and S. Mrenna, *A Study of SUSY signatures at the Tevatron in models with near mass degeneracy of the lightest chargino and neutralino*, *Phys.Rev.* **D62** (2000) 015002, [[hep-ph/9906270](#)].
- [60] J. F. Gunion and S. Mrenna, *Probing models with near degeneracy of the chargino and LSP at a linear $e^+ e^-$ collider*, *Phys.Rev.* **D64** (2001) 075002, [[hep-ph/0103167](#)].
- [61] A. Barr, C. Lester, M. A. Parker, B. Allanach, and P. Richardson, *Discovering anomaly mediated supersymmetry at the LHC*, *JHEP* **0303** (2003) 045, [[hep-ph/0208214](#)].
- [62] M. Ibe, T. Moroi, and T. Yanagida, *Possible Signals of Wino LSP at the Large Hadron Collider*, *Phys.Lett.* **B644** (2007) 355–360, [[hep-ph/0610277](#)].
- [63] M. R. Buckley, L. Randall, and B. Shuve, *LHC Searches for Non-Chiral Weakly Charged Multiplets*, *JHEP* **1105** (2011) 097, [[arXiv:0909.4549](#)].
- [64] ATLAS Collaboration, G. Aad et al., *Search for charginos nearly mass-degenerate with the lightest neutralino based on a disappearing-track signature in pp collisions at $\sqrt{s} = 8$ TeV with the ATLAS detector*, *Phys.Rev.* **D88** (2013) 112006, [[arXiv:1310.3675](#)].
- [65] M. Cacciari and G. P. Salam, *Pileup subtraction using jet areas*, *Phys.Lett.* **B659** (2008) 119–126, [[arXiv:0707.1378](#)].
- [66] D. Krohn, M. Low, M. D. Schwartz, and L.-T. Wang, *Jet Cleansing: Pileup Removal at High Luminosity*, [arXiv:1309.4777](#).
- [67] P. Berta, M. Spouta, D. W. Miller, and R. Leitner, *Particle-level pileup subtraction for jets and jet shapes*, [arXiv:1403.3108](#).
- [68] L. Randall and R. Sundrum, *Out of this world supersymmetry breaking*, *Nucl.Phys.* **B557** (1999) 79–118, [[hep-th/9810155](#)].
- [69] G. F. Giudice, M. A. Luty, H. Murayama, and R. Rattazzi, *Gaugino mass without singlets*, *JHEP* **9812** (1998) 027, [[hep-ph/9810442](#)].
- [70] K. Cheung and C.-W. Chiang, *Splitting split supersymmetry*, *Phys.Rev.* **D71** (2005) 095003, [[hep-ph/0501265](#)].
- [71] A. Arvanitaki, N. Craig, S. Dimopoulos, and G. Villadoro, *Mini-Split*, *JHEP* **1302** (2013) 126, [[arXiv:1210.0555](#)].

- [72] L. J. Hall and Y. Nomura, *Spread Supersymmetry*, *JHEP* **1201** (2012) 082, [[arXiv:1111.4519](#)].
- [73] L. J. Hall, Y. Nomura, and S. Shirai, *Spread Supersymmetry with Wino LSP: Gluino and Dark Matter Signals*, *JHEP* **1301** (2013) 036, [[arXiv:1210.2395](#)].
- [74] J. Hisano, S. Matsumoto, M. Nagai, O. Saito, and M. Senami, *Non-perturbative effect on thermal relic abundance of dark matter*, *Phys.Lett.* **B646** (2007) 34–38, [[hep-ph/0610249](#)].
- [75] T. Cohen, M. Lisanti, A. Pierce, and T. R. Slatyer, *Wino Dark Matter Under Siege*, *JCAP* **1310** (2013) 061, [[arXiv:1307.4082](#)].
- [76] J. Fan and M. Reece, *In Wino Veritas? Indirect Searches Shed Light on Neutralino Dark Matter*, *JHEP* **1310** (2013) 124, [[arXiv:1307.4400](#)].
- [77] Fermi-LAT collaboration, M. Ackermann et al., *Constraining Dark Matter Models from a Combined Analysis of Milky Way Satellites with the Fermi Large Area Telescope*, *Phys.Rev.Lett.* **107** (2011) 241302, [[arXiv:1108.3546](#)].
- [78] H.E.S.S. Collaboration, A. Abramowski et al., *Search for photon line-like signatures from Dark Matter annihilations with H.E.S.S.*, *Phys.Rev.Lett.* **110** (2013) 041301, [[arXiv:1301.1173](#)].
- [79] CTA Consortium, M. Actis et al., *Design concepts for the Cherenkov Telescope Array CTA: An advanced facility for ground-based high-energy gamma-ray astronomy*, *Exper.Astron.* **32** (2011) 193–316, [[arXiv:1008.3703](#)].
- [80] L. Bergstrom, G. Bertone, J. Conrad, C. Farnier, and C. Weniger, *Investigating Gamma-Ray Lines from Dark Matter with Future Observatories*, *JCAP* **1211** (2012) 025, [[arXiv:1207.6773](#)].
- [81] R. J. Hill and M. P. Solon, *WIMP-nucleon scattering with heavy WIMP effective theory*, [arXiv:1309.4092](#).
- [82] P. Cushman, C. Galbiati, D. McKinsey, H. Robertson, T. Tait, et al., *Snowmass CF1 Summary: WIMP Dark Matter Direct Detection*, [arXiv:1310.8327](#).
- [83] M. Ibe, S. Matsumoto, and R. Sato, *Mass Splitting between Charged and Neutral Winos at Two-Loop Level*, *Phys.Lett.* **B721** (2013) 252–260, [[arXiv:1212.5989](#)].
- [84] L. J. Hall, D. Pinner, and J. T. Ruderman, *A Natural SUSY Higgs Near 126 GeV*, *JHEP* **1204** (2012) 131, [[arXiv:1112.2703](#)].
- [85] M. Papucci, J. T. Ruderman, and A. Weiler, *Natural SUSY Endures*, *JHEP* **1209** (2012) 035, [[arXiv:1110.6926](#)].
- [86] N. Arkani-Hamed, S. Dimopoulos, and S. Kachru, *Predictive landscapes and new physics at a TeV*, [hep-th/0501082](#).
- [87] N. Arkani-Hamed, A. Delgado, and G. Giudice, *The Well-tempered neutralino*, *Nucl.Phys.* **B741** (2006) 108–130, [[hep-ph/0601041](#)].
- [88] K. L. Chan, U. Chattopadhyay, and P. Nath, *Naturalness, weak scale supersymmetry and the prospect for the observation of supersymmetry at the Tevatron and at the CERN LHC*, *Phys.Rev.* **D58** (1998) 096004, [[hep-ph/9710473](#)].
- [89] J. L. Feng, K. T. Matchev, and T. Moroi, *Focus points and naturalness in supersymmetry*, *Phys.Rev.* **D61** (2000) 075005, [[hep-ph/9909334](#)].

- [90] J. L. Feng, K. T. Matchev, and F. Wilczek, *Neutralino dark matter in focus point supersymmetry*, *Phys.Lett.* **B482** (2000) 388–399, [[hep-ph/0004043](#)].
- [91] J. L. Feng, K. T. Matchev, and D. Sanford, *Focus Point Supersymmetry Redux*, *Phys.Rev.* **D85** (2012) 075007, [[arXiv:1112.3021](#)].
- [92] S. Akula, M. Liu, P. Nath, and G. Peim, *Naturalness, Supersymmetry and Implications for LHC and Dark Matter*, *Phys.Lett.* **B709** (2012) 192–199, [[arXiv:1111.4589](#)].
- [93] C. Cheung, L. J. Hall, D. Pinner, and J. T. Ruderman, *Prospects and Blind Spots for Neutralino Dark Matter*, *JHEP* **1305** (2013) 100, [[arXiv:1211.4873](#)].
- [94] M. Cahill-Rowley, R. Cotta, A. Drlica-Wagner, S. Funk, J. Hewett, et al., *Complementarity and Searches for Dark Matter in the pMSSM*, [arXiv:1305.6921](#).
- [95] C. Cheung and D. Sanford, *Simplified Models of Mixed Dark Matter*, [arXiv:1311.5896](#).
- [96] K. Griest and D. Seckel, *Three exceptions in the calculation of relic abundances*, *Phys.Rev.* **D43** (1991) 3191–3203.
- [97] S. Profumo and C. Yaguna, *Gluino coannihilations and heavy bino dark matter*, *Phys.Rev.* **D69** (2004) 115009, [[hep-ph/0402208](#)].
- [98] D. Feldman, Z. Liu, and P. Nath, *Gluino NLSP, Dark Matter via Gluino Coannihilation, and LHC Signatures*, *Phys.Rev.* **D80** (2009) 015007, [[arXiv:0905.1148](#)].
- [99] K. Harigaya, K. Kaneta, and S. Matsumoto, *Gaugino coannihilations*, [arXiv:1403.0715](#).
- [100] A. De Simone, G. F. Giudice, and A. Strumia, *Benchmarks for Dark Matter Searches at the LHC*, [arXiv:1402.6287](#).
- [101] C. Boehm, A. Djouadi, and M. Drees, *Light scalar top quarks and supersymmetric dark matter*, *Phys.Rev.* **D62** (2000) 035012, [[hep-ph/9911496](#)].
- [102] T. Cohen and J. G. Wacker, *Here be Dragons: The Unexplored Continents of the CMSSM*, *JHEP* **1309** (2013) 061, [[arXiv:1305.2914](#)].
- [103] M. Carena, A. Freitas, and C. Wagner, *Light Stop Searches at the LHC in Events with One Hard Photon or Jet and Missing Energy*, *JHEP* **0810** (2008) 109, [[arXiv:0808.2298](#)].
- [104] J. R. Ellis, T. Falk, and K. A. Olive, *Neutralino - Stau coannihilation and the cosmological upper limit on the mass of the lightest supersymmetric particle*, *Phys.Lett.* **B444** (1998) 367–372, [[hep-ph/9810360](#)].
- [105] J. M. Lindert, F. D. Steffen, and M. K. Trenkel, *Direct stau production at hadron colliders in cosmologically motivated scenarios*, *JHEP* **1108** (2011) 151, [[arXiv:1106.4005](#)].
- [106] C. Rogan, *Kinematical variables towards new dynamics at the LHC*, [arXiv:1006.2727](#).
- [107] P. J. Fox, R. Harnik, R. Primulando, and C.-T. Yu, *Taking a Razor to Dark Matter Parameter Space at the LHC*, *Phys.Rev.* **D86** (2012) 015010, [[arXiv:1203.1662](#)].
- [108] M. R. Buckley, J. D. Lykken, C. Rogan, and M. Spiropulu, *Super-Razor and Searches for Sleptons and Charginos at the LHC*, *Phys.Rev.D* (2013) [[arXiv:1310.4827](#)].
- [109] G. P. Salam, *Perturbative QCD for the LHC*, *PoS ICHEP2010* (2010) 556, [[arXiv:1103.1318](#)].